Journal of
Applied Remote Sensing

Biweekly disturbance capture and attribution: case study in western Alberta grizzly bear habitat

Thomas Hilker
Nicholas C. Coops
Rachel Gaulton
Michael A. Wulder
Jerome Cranston
Gordon Stenhouse

Biweekly disturbance capture and attribution: case study in western Alberta grizzly bear habitat

Thomas Hilker,[a] Nicholas C. Coops,[b] Rachel Gaulton,[c] Michael A. Wulder,[d] Jerome Cranston,[e] and Gordon Stenhouse[e]

[a] NASA Goddard Space Flight Center, Biospheric Sciences Branch Code 618, Greenbelt, Maryland 20771
thomas.hilker@nasa.gov

[b] University of British Columbia, Faculty of Forest Resources Management, 2424 Main Mall, Vancouver, British Columbia, V6T 1Z4, Canada

[c] Newcastle University, Department of Civil Engineering and Geosciences, Newcastle upon Tyne, NE1 7RU, United Kingdom

[d] Canadian Forest Service (Pacific Forestry Centre), Natural Resources Canada, 506 West Burnside Road, Victoria, British Columbia, V8Z 1M5, Canada

[e] Foothills Research Institute, Hinton, Alberta, T7V 1X6, Canada

Abstract. An increasing number of studies have demonstrated the impact of landscape disturbance on ecosystems. Satellite remote sensing can be used for mapping disturbances, and fusion techniques of sensors with complimentary characteristics can help to improve the spatial and temporal resolution of satellite-based mapping techniques. Classification of different disturbance types from satellite observations is difficult, yet important, especially in an ecological context as different disturbance types might have different impacts on vegetation recovery, wildlife habitats, and food resources. We demonstrate a possible approach for classifying common disturbance types by means of their spatial characteristics. First, landscape level change is characterized on a near biweekly basis through application of a data fusion model (spatial temporal adaptive algorithm for mapping reflectance change) and a number of spatial and temporal characteristics of the predicted disturbance patches are inferred. A regression tree approach is then used to classify disturbance events. Our results show that spatial and temporal disturbance characteristics can be used to classify disturbance events with an overall accuracy of 86% of the disturbed area observed. The date of disturbance was identified as the most powerful predictor of the disturbance type, together with the patch core area, patch size, and contiguity.
 [DOI: 10.1117/1.3664342]

Keywords: disturbance mapping; disturbance attribution; Landsat; MODIS; change detection; temporal resolution; forest harvest; *Ursus arctos* L.

Paper 11101RR received Jun. 11, 2011; revised manuscript received Oct. 28, 2011; accepted for publication Nov. 7, 2011; published online Dec. 1, 2011.

1 Introduction

Natural and anthropogenic disturbances can have major impacts on biodiversity by fragmenting, reducing, or increasing edges of wildlife habitats and by increasing availability of open areas and associated food resources, such as emerging grasses and herbaceous plants.[1,2] For example, grizzly bear (Ursus arctos L.) habitats are influenced by the temporal and spatial distribution of disturbances within the bear home ranges[1,3] and as a result, wildfire, harvesting, urban expansion road development, mining, and oil and gas exploitation activities all have a potential impact on bear habitat use and survival.[4] Disturbed areas, such as fire scars, roadside verges,

1931-3195/2011/$25.00 © 2011 SPIE

and harvested forest areas, can provide high quality forage;[1,3] however, bears also experience increased mortality when using such areas, due to a higher risk of conflict with humans.[5]

Effective protection of wildlife habitats requires reliable mapping and classification of fine scale disturbances to provide up-to-date spatial coverage for the management and conservation of fauna species.[6] Through the use of remote sensing and modeling approaches, wide-scale observations of disturbances are becoming increasingly operational and reliable[7] and remote sensing observations are being used in a wide range of ecological studies.[8] In forested areas, stand replacing disturbances caused by fire, clear felling, wind throw, and changes in land use can be readily identified.[9,10] A number of recent studies have also demonstrated that more subtle disturbances associated with tree thinning, insect outbreaks, and changes in forest composition can be successfully mapped from finer spatial resolution (pixels sided 10 to 100 m) remote sensing satellites.[11] In particular, Landsat imagery, with a 30 m spatial resolution, is often used to monitor changes in land cover (Wulder et al. 2008) and to map ecosystem disturbance at landscape and continental scales.[12] While Landsat is limited by its lengthy revisit cycle (16 days) which can be markedly extended in regions with frequent cloud cover,[13,14] a combination of Landsat with imagery from sensors with complementary spatial and temporal characteristics can help overcome some of these restrictions. For instance, high spatial resolution imagery can be combined with high temporal resolution data from the moderate resolution imaging spectroradiometer (MODIS) to allow the generation of synthetic, Landsat-like, observations with high spatial (30 m) and temporal (potentially daily) resolution.[13,15] These techniques allow the explicit detection of disturbance events at spatial scales smaller than that of a MODIS pixel and at biweekly intervals.[15,16] In this study we utilize such a fusion approach, the spatial temporal adaptive algorithm for mapping reflectance change (STAARCH)[16] to derive disturbances over a 185 × 185 km study area in western Alberta, Canada. The STAARCH algorithm has the advantage over other data fusion techniques such as spatial and temporal adaptive reflectance fusion model (STARFM),[13] or enhanced spatial and temporal adaptive reflectance fusion model (ESTARFM),[17] that it explicitly accounts for a small to medium area sized disturbance [<5 ha (Ref. 18)], thereby mapping the time of disturbance and its spatial extent. We investigate a series of spatial and temporal rules which can be used to characterize the type of disturbances occurring on the landscape, with the ultimate goal of linking these disturbance types back to grizzly bear behavior and movements. The findings reported in this study will help to facilitate a more accurate mapping of disturbance events, time of occurrence, and disturbance types.

2 Methods

2.1 Alberta Grizzly Bear Habitat Study Area

Loss of the grizzly bear habitat is occurring throughout the northern United States and southern Canada (Ref. 4) with only 37% considered secure within the current park and conservation network.[19] This is a critical issue, especially in Alberta, where populations are low yet oil and gas exploration is increasingly changing the landscape, as is timber harvesting due to the mitigation in response to the current infestation of the mountain pine beetle.[2] As a component of the Alberta grizzly bear recovery plan, core (considered areas of high resources and low mortality risk) or secondary (areas with increased mortality risk) bear habitats have been defined. Mapping with attribution of key disturbance events within core and secondary habitats is a management imperative.[18]

A total of 42 Landsat 5 TM cloud-free scenes covering an area of 14 path/rows (Fig. 1), acquired between July and October 2001, June and August 2004, and July and September 2008 were available for the entire study area and obtained from the USGS GLOVIS archive (http://glovis.usgs.gov/).[18] Images were selected to minimize cloud cover (where possible to below 30%) and the temporal separation between adjacent scenes across the study area. All images were atmospherically corrected using a dark object subtraction.[18] MODIS 8-day composites from 2001 to 2008 were also acquired for the entire area and re-projected to the

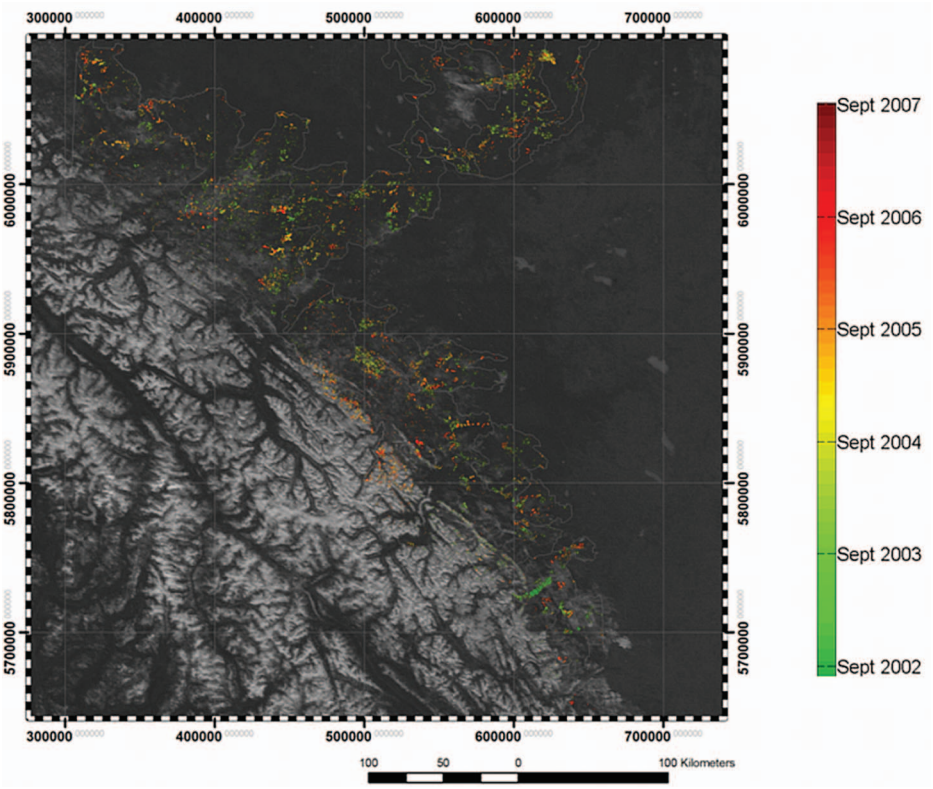

Fig. 1 Bimonthly disturbance map of the study area in southern Alberta derived from STAARCH on the backdrop of a MODIS images. The highlighted areas in the image correspond to the DoD, spatial coordinates are provided in UTM, Zone 11 (See Ref. 18 for details).

Universal Transverse Mercator (UTM) projection using the MODIS re-projection tool, clipped to the extent of the Landsat imagery and re-sampled to a 30 m spatial resolution. Land cover data was obtained from the Landsat-7 land cover classification of Canada that was produced for the Earth Observation for Sustainable Development of Forests initiative,[20] representing circa year 2000 conditions.

2.2 Detection of Landscape Disturbance

STAARCH is a change detection algorithm designed to map forest disturbance events at a 30 m spatial resolution and at weekly or biweekly time intervals.[16] The spatial extent of a given disturbance can be determined from any two Landsat scenes acquired before and after the disturbance event: The change detection in STAARCH utilizes a disturbance index[11] derived from a tasselled cap transformed image space of each of the two Landsat scenes.[21] The date of disturbance (DoD) for each disturbed area is then determined from a time series of MODIS images acquired at weekly or bimonthly intervals; a detailed description can be found in Hilker et al.[16] The two main outputs of STAARCH are 1. a spatial change mask of forest disturbance at 30 m spatial resolution and 2. a MODIS image sequence representing the temporal evolution of these disturbance events. Change predictions are restricted to the vegetation season (mid-March to mid-October) and cloud-free areas with clouds detected automatically using a Landsat-based cloud filter.[22] In this study we utilized STAARCH derived disturbance data over 150,000 ha in the study area in west-central Alberta mapping disturbances in bimonthly intervals between June 2001 and August 2008 (Ref. 18, Fig. 1). The STAARCH algorithm was implemented separately on each Landsat path/row to produce 14 disturbance sequences. Once combined, the sequences

serve to collectively cover the majority of the Alberta grizzly bear core and secondary habitat area, with change predictions made at 16 day time steps.

2.3 Determining the Type of Disturbance from Spatial Characteristics

The aim of this analysis was to determine the type of disturbance from the spatial characteristics of individual disturbance events. Landscape pattern indices can be grouped into categories of size, shape index (edge-to-area ratio), isolation/proximity, and contagion/interspersion.[23] Critical indices in forested environments undergoing disturbance, based on a previous review,[24] include the number of patches per unit area, size class, and area-weighted mean patch size. In concert with edge density, these indices provide an indication of the degree of fragmentation associated with the different disturbance events. Conversely, area-weighted mean fractal dimension, mean proximity index, and interspersion/juxtaposition index provide a means to characterize patch shape, patch isolation/proximity, and contagion/interspersion, respectively.[24]

Patch analysis of the disturbed areas was undertaken using Fragstats, a software tool designed to compute a wide variety of landscape metrics for categorical maps.[23] Pixels flagged as disturbed were converted into disturbance patches by connecting adjacent pixels with the same disturbance date and growing the area until no more adjacent pixels were found. The patches were then converted to polygons and those with an area of less than 1 ha were removed, as STAARCH does not well predict changes below 1 ha.[18] Fragstats computes disturbance characteristics based on a number of patch characteristics. These fragstats characteristics can be broadly categorized as area/density/edge metrics, shape metrics, core metrics, isolation/proximity metrics, contrast metrics, contagion/interspersion metrics, connectivity metrics, and diversity metrics.[25] In this study, we characterized the disturbed areas identified by STAARCH using 19 different Fragstats derived metrics including area, perimeter, radius of gyration, number of patches, patch density, edge density, landscape shape index, largest patch index, perimeter-area ratio, shape index, continuity index, fractal dimension index, linearity index, circumscribing circle, core area, number of disjunct core areas in each patch, isolation/proximity, Euclidean nearest neighbor (see Help Content of Fragstats for further information and definition). In addition to these spatial categories, the high temporal density of the STAARCH-based output also allowed us to use the disturbance date as an additional characteristic.

The disturbance characteristics which best predicted the types of disturbance were identified using decision tree analysis. This nonparametric approach serves to automatically separate the dependent variables (spatial and temporal disturbance characteristics) into a series of choices that not only identifies the importance of each constraining variable but also identifies thresholds that best separate one class from another and best explain the response variable (here: disturbance type). One advantage of using decision trees over conventional regression techniques is its capacity to deal with collinear datasets, to exclude insignificant variables and its independence of dataset distributions such as asymmetrical distribution of samples.[26,27] Decision Tree Regression software was used to develop a classification tree for each disturbance type using a 10-fold cross validation technique where the total dataset is partitioned randomly into 10 equally sized groups, a model is developed on 9 of the groups, and then tested against the remaining 10% of the data not used in model development. Tree pruning was set to the minimum cross validation error and a maximum tree depth of six levels was defined to prevent overly complex model results.

A disturbance type map for validation was available which had been derived from visual interpretation undertaken by a trained aerial photographic analyst familiar with the region. Air photo interpretation was based on maps of fire history, harvesting records, and road coverage. For demonstration of our technique, we used the most common disturbance types occurring in the study area: cut blocks, fires, roads, and well sites. Photointerpreted patches were matched to STAARCH-detected patches by assigning the disturbance type of the patch with the largest common area of overlap. A total of 189 disturbance patches identified by the photointerpreter were used as the training dataset.

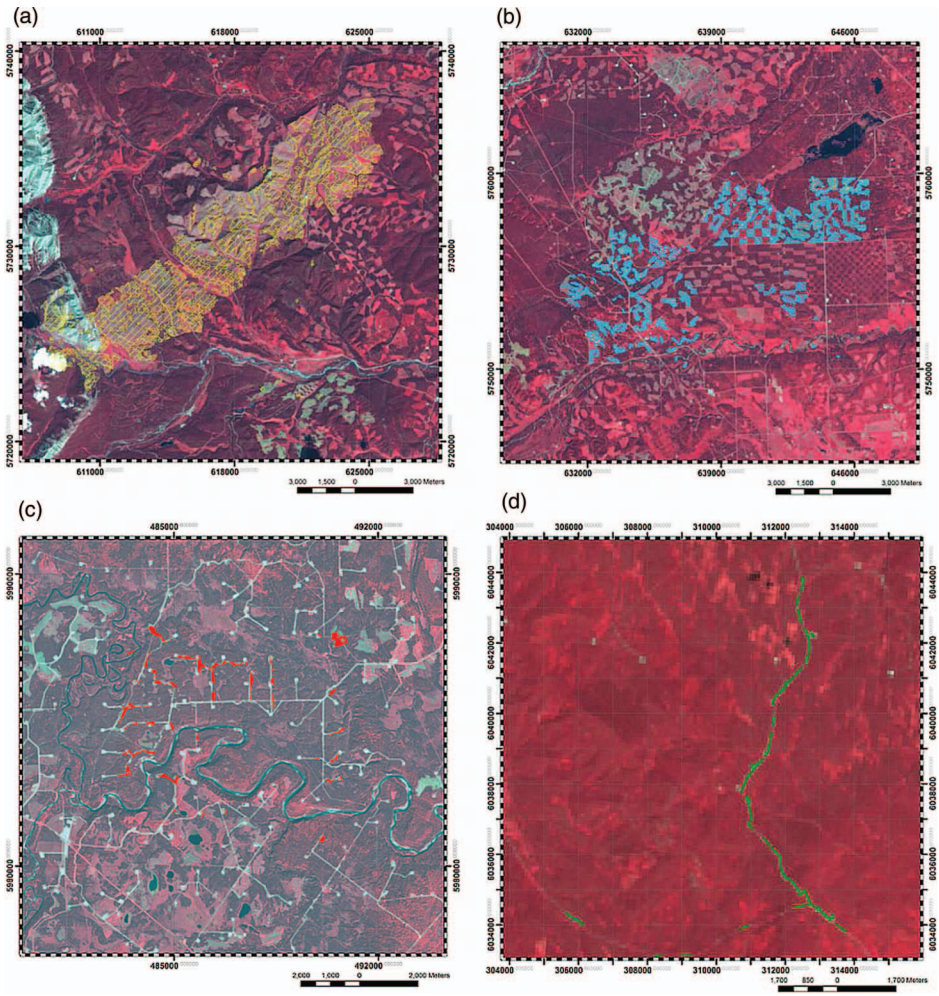

Fig. 2 Spatial characteristics of the most important types of disturbances occurring in the study area. Dogrib Creek Fire (a), harvesting cut blocks (b), well sites (c), and roads (d).

3 Results

Figure 2 illustrates examples of different types of disturbances examined in the study area. Figure 2(a) shows the Dogrib Creek Fire, which burned from September to October, 2001 in an area of 787.8 ha.[18] Burns were primarily characterized by large, contiguous patch sizes (>4.5 ha). An example of cut blocks is provided in Fig. 2(b). The highlighted areas in the image show harvesting activities since 2001, the other patches are disturbances that have occurred prior to this date and have been ignored in this study. Cut blocks were characterized by a regular shape and "checkerboard" configuration, typically around 25 to 50 ha in size. Well sites [Fig. 2(c)] were characterized by the attachment to short access roads and smaller, rectangular disturbance patches, whereas roads were determined mainly by their long and comparatively narrow shapes [Fig. 2(d)].

The classification tree resulting from fitting the different disturbance types to the patch metrics derived from Fragstats is presented in Fig. 3. The tree depth was restricted to 6 levels and the tree was pruned to its minimum cross validation error. The overall classification accuracy was 86.17%, based on the total area disturbed; the sensitivity and specificity statistics for each disturbance type is provided in Table 1. The sensitivity describes the proportion of positives correctly classified as such. Specificity describes the proportion of negatives which are correctly

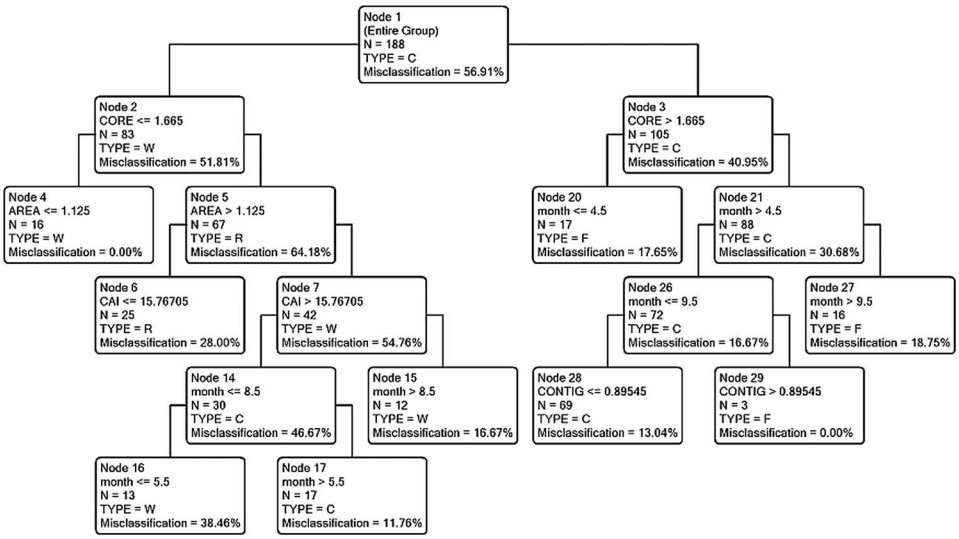

Fig. 3 Classification tree for classifying the type of disturbance from spatial area metrics of the disturbed areas derived from Fragstats (see Table 3 for a legend and explanation).

identified. The misclassification errors ranged between 20% and 30% for cut blocks, fires, and well sites, whereas roads were misclassified more often (60%). The accuracies for the individual disturbance types ranged between 83% and 89%, while the precision ranged between 58% and 82%. Lowest precision values were found for roads, which also showed the highest rate of misclassification. About 20% of pixels had multiple events with an earlier event assigned as the disturbance date.

Table 2 shows the confusion matrix for cut blocks, fires, well sites, and roads. Most common misclassifications occurred between fires and cut blocks and between roads and well sites. The producer's accuracy for the four different disturbance classes ranged between 56% and 79%, while the user's accuracy was lowest for roads (40%), and highest for cut blocks (80%). The overall accuracy resulting from the confusion matrix was 67%; please note, however, that the amount of total area correctly identified is higher (86%) as the confusion matrix does not take the differences in percent area covered by each disturbance class into account. Regression tree analysis was successfully used to extract the most important spatial and temporal characteristics from the set of variables computed by STAARCH and Fragstats. A ranking of the shape metrics and disturbance characteristics that were used to characterize the different types of disturbance is presented in Table 3. The importance of values is scaled between 100 (most important) and 0 (not important). The most important metrics for classifying the disturbances was the month of disturbance as identified from the STAARCH algorithm, followed by the core (interior) area of the disturbed patch and the disturbance size. Core area index and contiguity both describe the shape of the disturbance by comparing the disturbed core area to the disturbance perimeter. It should be noted that no STAARCH predictions were made outside the growing season due to possible snow contamination, and, as a result, disturbance events occurring after October 15th were assigned the disturbance date of the first prediction of the following year (March 15th).

4 Discussion

This study demonstrated a possible approach for mapping disturbance types through automated detection and classification of disturbance events derived from a data fusion model. Techniques like this are particularly important for habitats associated with rare species, such as grizzly bears, given the difficulty of repeatedly visiting remote sites at the frequency and quality

Table 1 Sensitivity and specificity analysis of the predicted disturbance types derived from classification tree analysis.

Category	Accuracy (%)	Sensitivity (%)	Specificity (%)	Geometric mean (%)	Precision (%)	Recall (%)	Misclassified (%)	F-statistics
Cut block(C)	84.04	80.25	86.92	83.51	82.28	82.25	19.75	0.8125
Fire (F)	89.36	76.32	92.67	84.09	72.50	76.32	23.68	0.7436
Road (R)	88.30	40.00	95.71	61.87	58.82	40.00	60.00	0.4762
Well site (W)	82.98	72.73	86.11	79.14	61.54	72.73	27.27	0.6667

Table 2 Confusion matrix of the predicted (rows) and observed (columns) disturbance types (values in% area).

Category	Cut block (C)	Fire (F)	Road (R)	Well site (W)	User's accuracy
Cut block (C)	80.25	7.41	2.47	9.88	0.80
Fire (F)	23.68	76.32	0.00	0.00	0.76
Road (R)	8.00	4.00	40.00	48.00	0.40
Well site (W)	6.82	9.09	11.36	72.73	0.72
Producer's accuracy	0.68	0.79	0.74	0.56	

necessary for detecting changes in critical food resources.[28] While this research described an approach for the classification of automatically detected disturbance events, further research will be required to determine disturbance types that are of key importance for grizzly bear movements and habitat use, both in terms of short and long term response[18] and eventually link these disturbance types back to bear population and bear ecology. For instance, the temporal distribution and patch size of disturbance events appears to be influenced by the dominant disturbance type with small patches resulting from harvesting and much larger areas being disturbed by wildfires. The least disturbed areas were often located in areas away from road networks and at high elevations. These are also areas that contain large proportions of core grizzly bear habitat in conservation areas.[1,3,4] Further research is needed also to link the cause and the time of disturbance to grizzly bear movement and the presence in given areas in order to minimize the impact of such events on the bear population. Also, improvement of detecting the disturbance type in heterogeneous landscapes could potentially be reached by combining the ESTARFM (Ref. 17) approach with the STAARCH-based disturbance detection, as ESTARFM was designed to improve the prediction accuracy especially in heterogeneous landscapes. One limitation of STAARCH, besides cloud contamination, is its restriction to observations made only during the growing season.[17,18] This limitation, which was implemented to avoid prediction inaccuracies due to snow cover, is less relevant in the context of mapping grizzly bear habitats due to the dormancy of the bears; however, it may cause inaccuracies in that disturbance events from outside the growing season will be assigned the date of first Landsat observation of the following growing season.[17,18] This was documented,[18] for instance, for parts of the Dogrib Creek Fire, which burned in October 2001 but was assigned a disturbance date of early 2002, as this was to the first MODIS used after this event.

Table 3 Spatial disturbance attributes (Fragstats) and their predictive power derived from classification tree analysis.

Metrics name	Importance	Description
DoD	100.00	**Date of Disturbance:** STAARCH derived bimonthly disturbance interval
Core (m^2)	70.12	**Core Area: Area (m^2):** area within the patch that is further than the specified depth-of-edge distance (here 30 m) from the patch perimeter
Area (m^2)	22.58	**Patch area:** The area of the patch in m^2
CAI	22.17	**Core Area Index.** Patch core area (m^2) divided by total patch area (m^2), multiplied by 100 (to convert to a percentage); in other words, CAI equals the percentage of a patch that is core area.
Contig	12.46	**Contiguity Index:** The average contiguity value for the cells in a patch (i.e., sum of the cell values (= 1 for the binary disturbance mask) divided by the total number of pixels in the patch) minus 1, divided by the sum of the template values (= 1) minus 1. Note, 1 is subtracted from both the numerator and denominator to confine the index to a range of 1.

The selected technique was particularly successful in distinguishing between disturbances with more compact shapes, such as cut blocks or fires and stretched disturbance types, which typically represented an access road or other linear feature such as pipeline right-of-way. These disturbance types were classified correctly in 60% to 70% of the cases (Table 1) and little to almost no confusion was found between these two disturbance types (Table 2). This is also reflected in the predictive power of the individual variables shown in Table 3. Most of the disturbance metrics were related to the compactness of the area, area size, and shape. Additionally, the contiguity of the disturbance patches was identified as a significant predictor of the type of disturbance. The high ranking of the date of disturbances demonstrates the usefulness of the STAARCH algorithm not only to predict the temporal sequence of individual disturbance events but also to classify the disturbance type. A potential explanation for the significance of this metric is the increased harvesting and mining activity during the growing season, which will also lead to increased disturbances due to road construction during this time. Likewise, forest fires occur predominantly during drier periods, thereby providing an opportunity for automatic classification of this disturbance type[18] (in combination with shape characteristics). Misclassifications were found mainly for disturbances related to road construction. Most commonly misclassified as well sites (Table 2), both classes have similar spatial characteristics with long and thin shapes (Fig. 2). Many well site patches were merged with the associated spur road, which is another explanation for the higher misclassification rate. Additionally, road disturbances were only a few Landsat pixels wide, and as a result, the coherent disturbances were often patched into multiple disturbance polygons, such as shown in Fig. 2(d), which may explain the higher rate of misclassification as segments have different shapes and sizes than an unbroken feature would have. Often, road polygons occurred where the road widened, such as a junction or borrow pit. Classification tree analysis was used successfully to classify the disturbance patches according to their spatial and temporal characteristics. One of the potential limitations of classification and regression trees is overfitting of the model and complexity of the resulting tree model. While in this study a simple threshold was used to prune the tree to a depth of 5 levels maximum, future research could make use of other robust techniques such as decision tree forests or random forest approaches.

The results presented in this work will inform the development of new classification algorithms that will allow the prediction of disturbance types over large areas and from automated remote sensing approaches.

Acknowledgments

Funding for this research was generously provided by the Grizzly Bear Program of the Foothills Research Institute located in Hinton, Alberta, Canada, with additional information available at: http://www.fmf.ab.ca/. Additional funding provided through an NSERC grant to Coops, and to Wulder through the Canadian Forest Service (CFS).

References

1. A. Berland, T. Nelson, G. Stenhouse, K. Graham, and J. Cranston, "The impact of landscape disturbance on grizzly bear habitat use in the Foothills Model Forest, Alberta, Canada," *Forest Ecol. Manage.* **256**(11), 1875–1883 (2008).
2. J. Linke, S. E. Franklin, F. Huettmann, and G. B. Stenhouse, "Seismic cutlines, changing landscape metrics and grizzly bear landscape use in Alberta," *Landscape Ecol.* **20**(7), 811–826 (2005).
3. C. L. Roever, M. S. Boyce, and G. B. Stenhouse, "Grizzly bears and forestry – II: Grizzly bear habitat selection and conflicts with road placement," *Forest Ecol. Manage.* **256**(6), 1262–1269 (2008).

4. S. E. Nielsen, M. S. Boyce, and G. B. Stenhouse, "Grizzly bears and forestry I. Selection of clearcuts by grizzly bears in west-central Alberta, Canada," *Forest Ecol. Manage.* **199**(1), 51–65 (2004).
5. T. M. McLellan, M. E. Martin, J. D. Aber, J. M. Melillo, K. J. Nadelhoffer, and B. Dewey, "Comparison of wet chemistry and near infrared reflectance measurements of carbon fraction chemistry and nitrogen concentration of forest foliage," *Can. J. Forest Res.* **21**(11), 1689–1693 (1991).
6. S. L. Ustin, A. A. Gitelson, S. Jacquemoud, M. Schaepman, G. P. Asner, J. A. Gamon, and P. Zarco-Tejada, "Retrieval of foliar information about plant pigment systems from high resolution spectroscopy," *Remote Sens. Environ.* **113**, S67–S77 (2009).
7. P. Coppin, I. Jonckheere, K. Nackaerts, B. Muys, and E. Lambin, "Digital change detection methods in ecosystem monitoring: arReview," *Int. J. Remote Sens.* **25**(9), 1565–1596 (2004).
8. W. Cohen and S. Goward, "Landsat's role in ecological applications of remote sensing," *BioScience* **54**(6), 535–545 (2004).
9. G. Foody, R. Lucas, P. Curran, and M. Honzak, "Estimation of the areal extent of land cover classes that only occur at a sub-pixel level," *Canadian J. Remote Sens.* **22**(4), 428–432 (1996).
10. E. Rignot, W. A. Sala, and D. L. Skole, "Mapping deforestation and secondary growth in Rondonia, Brazil, using imaging radar and Thematic Mapper data," *Remote Sens. Environ.* **59**, 167–179 (1997).
11. S. P. Healey, W. B. Cohen, Z. Q. Yang, and O. N. Krankina, "Comparison of Tasseled Cap-based Landsat data structures for use in forest disturbance detection," *Remote Sens. Environ.* **97**(3), 301–310 (2005).
12. J. G. Masek, C. Q. Huang, R. Wolfe, W. Cohen, F. Hall, J. Kutler, and P. Nelson, "North American forest disturbance mapped from a decadal Landsat record," *Remote Sens. Environ.* **112**(6), 2914–2926 (2008).
13. F. Gao, J. Masek, M. Schwaller, and F. Hall, "On the blending of the Landsat and MODIS surface reflectance: Predicting daily Landsat surface reflectance," *IEEE Trans. Geosci. Remote Sens.* **44**(8), 2207–2218 (2006).
14. D. P. Roy, J. Ju, P. Lewis, C. Schaaf, F. Gao, M. Hansen, and E. Lindquist, "Multi-temporal MODIS-Landsat data fusion for relative radiometric normalization, gap filling, and prediction of Landsat data," *Remote Sens. Environ.* **112**(6), 3112–3130 (2008).
15. T. Hilker, M. A. Wulder, N. C. Coops, N. Seitz, J. C. White, F. Gao, J. G. Masek, and G. Stenhouse, "Generation of dense time series synthetic Landsat data through data blending with MODIS using a spatial and temporal adaptive reflectance fusion model," *Remote Sens. Environ.* **113**(9), 1988–1999 (2009).
16. T. Hilker, M. A. Wulder, N. C. Coops, J. Linke, G. McDermid, J. G. Masek, F. Gao, and J. C. White, "A new data fusion model for high spatial- and temporal-resolution mapping of forest disturbance based on Landsat and MODIS," *Remote Sens. Environ.* **113**(8), 1613–1627 (2009).
17. X. L. Zhu, J. Chen, F. Gao, X. H. Chen, and J. G. Masek, "An enhanced spatial and temporal adaptive reflectance fusion model for complex heterogeneous regions," *Remote Sens. Environ.* **114**(11), 2610–2623 (2010).
18. R. Gaulton, T. Hilker, M. A. Wulder, N. C. Coops, and G. Stenhouse, "Characterizing stand-replacing disturbance in western Alberta grizzly bear habitat, using a satellite-derived high temporal and spatial resolution change sequence," *Forest Ecol. Manage.* **261**(4), 865–877 (2011).
19. V. Banci, D. A.Demarchi , and W. R. Archibald, "Evaluation of the population status of grizzly bears in Canada," *Int. Conf. Bear Res. Manage.* **9**(1), 129–142 (1994).
20. M. A. Wulder, J. C. White, S. N. Goward, J. G. Masek, J. R. Irons, M. Herold, W. B. Cohen, T. R. Loveland, and C. E. Woodcock, "Landsat continuity: Issues and opportunities for land cover monitoring," *Remote Sens. Environ.* **112**(3), 955–969 (2008).

21. R. Kauth and G. Thomas, "The tasselled cap—A graphical description of the spectraltemporal development of agricultural crops as seen by Landsat," *Proceedings of the Symposium on Machine Processing of Remotely Sensed Data*, Purdue University Press, West Lafayette, Indiana, pp. 4B-414–B-51.
22. R. R. Irish, J. L. Barker, S. N. Goward, and T. Arvidson, "Characterization of the Landsat-7 ETM+automated cloud-cover assessment (ACCA) algorithm," *Photogramm. Eng. Remote Sens.* **72**(10), 1179–1188 (2006).
23. K. McGarigal and B. Marks, "FRAGSTATS: Spatial pattern analysis program for quantifying landscape structure," U.S. Dept. of Agriculture, Pacific Northwest Research Station (1998).
24. S. N. Gillanders, N. C. Coops, M. A. Wulder, S. E. Gergel, and T. Nelson, "Multitemporal remote sensing of landscape dynamics and pattern change: Describing natural and anthropogenic trends," *Prog. Phys. Geogr.* **32**(5), 503–528 (2008).
25. C. Su, B. Fu, Y. Lu, N. Lu, Y. Zeng, A. He, and H. Lamparski, "Land use change and anthropogenic driving forces: A case study in Yanhe River Basin," *Chin. Geogr. Sci.* **21**(5), 587–599 (2011).
26. G. De'ath and K. E. Fabricius, "Classification and regression trees: A powerful yet simple technique for ecological data analysis," *Ecology* **81**(11), 3178–3192 (2000).
27. C. R. Schwalm, T. A. Black, B. D. Arniro, M. A. Arain, A. G. Barr, C. P. A. Bourque, A. L. Dunn, L. B. Flanagan, M. A. Giasson, P. M. Lafleur, H. A. Margolis, J. H. McCaughey, A. L. Orchansky, and S. C. Wofsy, "Photosynthetic light use efficiency of three biomes across an east-west continental-scale transect in Canada," *Agric. Forest Meteorol.* **140**(1–4), 269–286 (2006).
28. C. W. Bater, M. A. Wulder, J. C. White and N. C. Coops, "Integration of LIDAR and digital aerial imagery for detailed estimates of Lodgepole Pine (Pinus contorta) volume killed by Mountain Pine Beetle (*Dendroctonus ponderosae*)," *J. For.* **108**(3), 111–119 (2010).

Biographies and photographs of the authors not available.